Stress and strain dependencies of shear modulus from pressuremeter tests in Opalinus Clay

Lang Liu
University of Alberta, Edmonton, Canada, lliu@ualberta.ca

Silvio Giger
Nationale Genossenschaft für die Lagerung radioaktiver Abfälle (NAGRA), Wettingen, Switzerland, silvio.giger@nagra.ch

Derek Martin[1], Rick Chalaturnyk[2], Nathan Deisman[3]
University of Alberta, Edmonton, Canada,

derek.martin@ualberta.ca[1], rc11@ualberta.ca[2], ndeisman@ualberta.ca[3]

ABSTRACT: Pre-bored pressuremeter tests were conducted in the Opalinus Clay at Mont Terri Rock Laboratory. The objective of the tests was to quantify the in-situ rock stiffness at multiple pressure levels. Tests in two boreholes by different types of pressuremeter probes both demonstrate high quality of field measurement. Both stress and strain dependencies of pressuremeter shear modulus are derived and assessed under undrained condition. It can be shown from the variation of pressuremeter shear modulus with stress applied at the borehole wall that the rock stiffness is gradually recovered as the load increases. This observed stress dependency may be further explained through a constitutive study of stiffness evolution under the stress/strain path relevant to pressuremeter testing.

Keywords: Pressuremeter Test; Shear Modulus; Opalinus Clay; Stress and strain dependencies.

1. Introduction

The Mont Terri Rock Laboratory, located in Northwest Switzerland is an underground research site for examining the potential of Opalinus Clay as host rock for radioactive waste disposal [1]. The Opalinus Clay exhibits geotechnical properties that are generally associated with "clay shale", as discussed by Morgenstern [2] and Gens [3]. Some of these properties, such as low permeability and swelling upon intake of moisture, are considered desirable for nuclear waste isolation.

Opalinus Clay was first deposited around 174 Ma ago. It then experienced a process of gradual burial and diagenesis which resulted in highly oriented clay fabrics. The present thickness of the Opalinus Clay in the laboratory is about 131m. Depending on the difference in mineral compositions, Opalinus Clay can be subdivided into three lithofacies – shaly, sandy and carbonate-rich sandy facies [1].

In the vicinity of an underground opening, Opalinus Clay is susceptible to damage induced from mechanical unloading and environmental changes after excavation. To characterize tunnel deformation and the development of excavation damage zone (EDZ), Amann et al. [4] investigated geomechanical behavior of Opalinus Clay at different scales. Determination of geomechanical parameters of Opalinus Clay is subject to a number of factors, including saturation condition, applied stress level and inherent material anisotropy [5-7]. Laboratory studies of the Opalinus Clay have been challenged by the difficulty of restoring in-situ condition after unloading. This can often lead to highly variable strength and stiffness parameters when obtained from core specimens [8, 9].

With the objective of determining the in-situ Opalinus Clay stiffness, pre-bored pressuremeter tests were completed in the Mont Terri Rock Laboratory. The pressuremeter tests were carried out using two types of probes (Fig. 1). Unload and reload cycles at multiple stress levels were performed in these tests. The results from the two series of tests are both considered to provide high quality field measurement. In this paper the observed nonlinear stress-strain behavior from the tests is analyzed. The stress dependency of the shear modulus is also assessed.

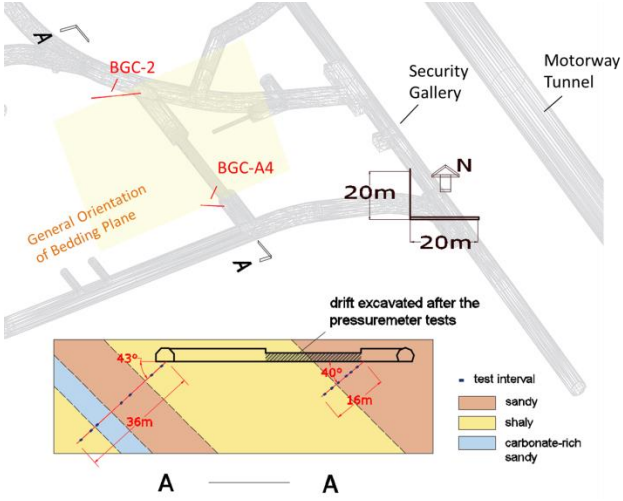

Figure 1. Location of two test boreholes in the Mont Terri Rock Laboratory

2. Two Pressuremeter Test Series

For these two series of tests, both boreholes were drilled perpendicular to the bedding plane and went

through different facies of Opalinus Clay (Fig.1). This means the pressure was applied in the direction parallel to the bedded clay particles. This test orientation should provide the minimum effect of structural anisotropy of the Opalinus Clay over the test intervals. Drilling was driven by air flush and was completed less than 2 days before pressuremeter tests were initiated. High-resolution borehole seismic survey was performed before the tests to confirm the Opalinus Clay facies at the test depths and avoid any highly fractured/collapsed zones that could damage the pressuremeter. A summary of the test details is given in Table 1.

Table 1. Two series of pressuremeter tests in Opalinus Clay at Mont Terri Rock Laboratory

Test Sequence	Test Depth	Facies	Maximum Test Pressure
Borehole BGC-2 (by SolExpert)			
#1	34.0m	Shaly	16.0MPa
#2	30.0m	Shaly	3.5MPa
#3	27.5m	Carbonate-rich Sandy	3.5MPa
#4	18.0m	Sandy	3.5MPa
#5	14.5m	Sandy	3.5MPa
#6	6.0m	Shaly	3.5MPa
#7	2.0m	Shaly	3.5MPa
Borehole BGC-A4 (by UofA)			
#1	14.9m	Shaly	18.0MPa
#2	12.2m	Shaly	14.0MPa
#3	9.7m	Sandy	14.0MPa
#4	2.5m	Sandy	13.9MPa
#5	6.7m	Sandy	15.7MPa
#6	4.9m	Sandy	17.4MPa

2.1. Tests in Borehole BGC-2

The first series of tests were conducted in borehole BGC-2 with SolExperts' pressuremeter probe (Fig. 2). The probe has three diametric displacement transducers, oriented at an angle of 120° to each other and placed in three planes spaced 75 mm apart (Fig. 2). With the steel pins penetrating through the packer membrane, the external deformation (at the borehole wall) can be directly measured. The transducers for diametric displacement measurement have a resolution of ±1 μm, allowing the rock stiffness to be determined at very small shear strains. Stiff tubing was used to install the probe and maintain its orientation in the borehole.

In each test, a base load of about 0.5 MPa was applied initially to obtain an even contact of the packer sleeve to the borehole wall. The load was then increased in 0.2 MPa steps in all the tests except the last one. The pressure was held for 3 minutes after each step. In the unload and reload cycles the pressure was held for 1 minute after a 0.45MPa pressure change. The stepwise control of pressure with time is shown in Fig.3.

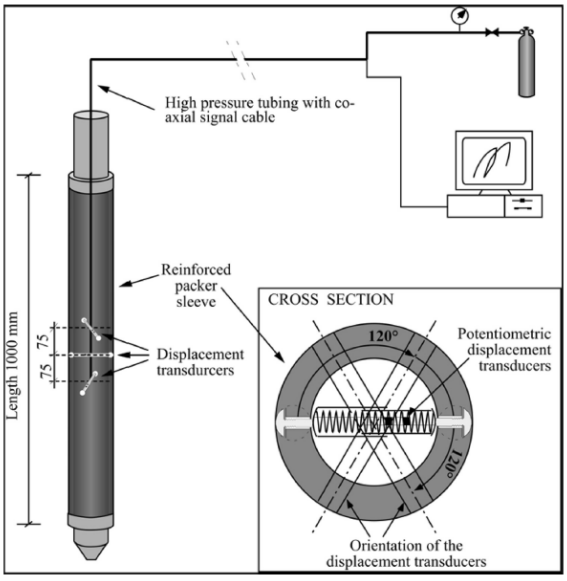

Figure 2. Schematic diagram of SolExperts' pressuremeter probe [10]

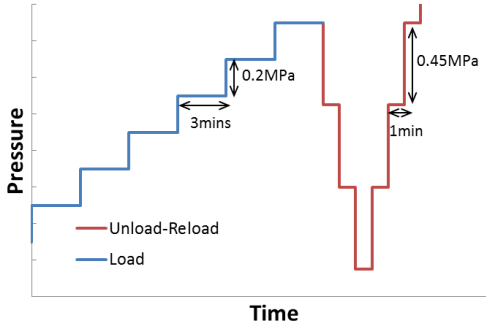

Figure 3. Typical pressure control for tests in borehole BGC-2

Fig.4 is an example plot of data obtained from Test #2 in borehole BGC-2. The radial displacement was zeroed by the first reading from the transducers so that the true diametric borehole deformation can be observed. The difference among three curves reveals the anisotropy of stiffness in the testing plane.

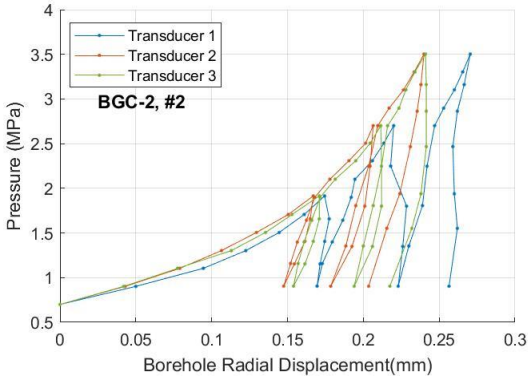

Figure 4. Typical test curves from tests in borehole BGC-2

In this dataset, transducer 1 captured an unsuual borehole deformation during all the unloads and reloads. Geological mapping of the core from the test interval indicated a strutural plane dipping through the planes where the transducers were located (Fig. 5). It is thus speculated that the unusual unload/relaod readings from transducer 1 were influenced by this local geologcial feature.

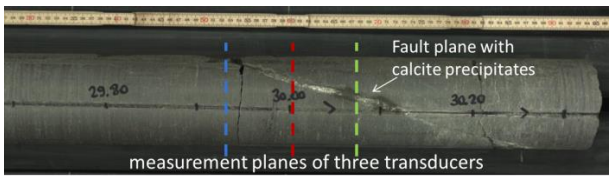

Figure 5. Core of shaly facies recovered from the test section of BGC-2, #2

An averaging procedure is applied to the measured dispalcement readings (Fig. 6). Compared with the curve averaged from all three transducer readings, the curve averaged from only tranducers 2 and 3 has a more reasonable unload-reload response and will be used in later analysis.

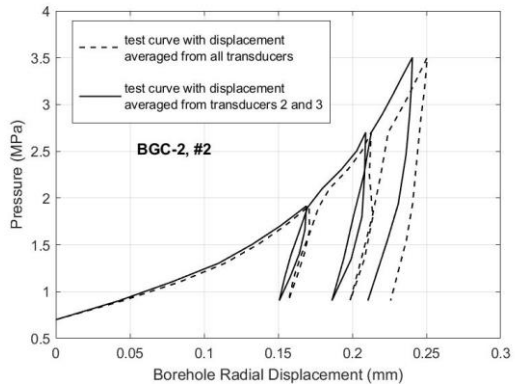

Figure 6. Test curves with averaged displacement reading

2.2. Tests in Borehole BGC-A4

The University of Alberta (UofA) performed another series of pressuremeter tests with the high pressure dilatometer (HPD) originally designed by Cambridge Insitu, Ltd. It has six independent radial caliper arms sitting on the same plane and 60° apart (Fig. 7). All the caliper arms are mechanically linked to strain gauges resolving displacements of less than ± 0.5 μm over a range of 16mm.

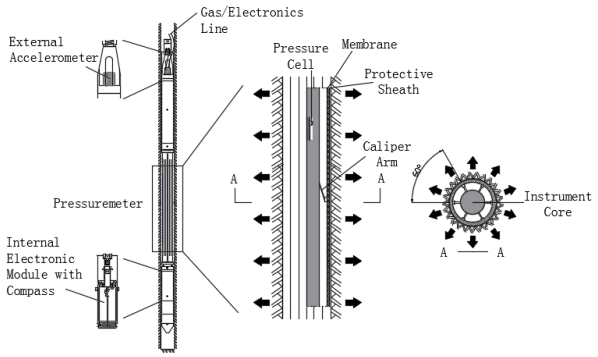

Figure 7. Schematic diagram of UofA's pressuremeter probe

The pressuremeter probe was deployed with wireline through a winch system. The orientation of the probe was determined by readings from an accelerometer attached at the instrument head.

For these tests the pressure was increased at the rate of about 300 kPa/min for most of the tests (Fig. 8). The unload rate ranged between 150 and 300 kPa/min, except in the last three unload-reload cycles in Tests #2 and #3, where unload rates were about 600 kPa/min. In addition, prior to unloading, the pressure was held constant for approximately 5 minutes, to minimize the

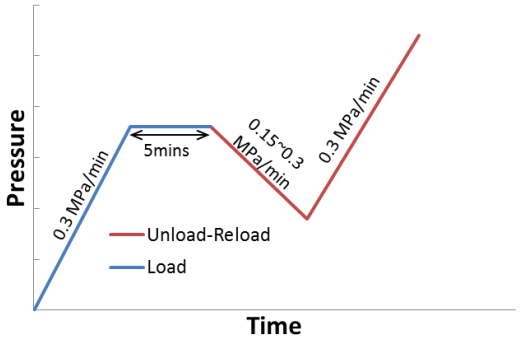

Figure 8. Typical pressure control for tests in borehole BGC-A4

influence of any excess pore pressure and creep on the subsequent deformation.

The UofA's probe was suspended on the wireline in the inclined borehole and consequently inflated during testing. The measured displacements of caliper arms were affected by the eccentric movement of the instrument core, and therefore were not the borehole deformation (Fig. 9). Two approaches can be used to minimize this effect: 1) average the pair of measurements on the same axis; and/or 2) correct the displacements by finding the relative movement of instrument center with respect to borehole for each pressure increment.

The first approach simply collapses the six radial measurements into three diametric measurements. The second approach preserves azimuthal information of each individual reading, but a fitting procedure must be applied over the data. This fitting procedure can result in over-smoothing the data. For this work the six readings are averaged arithmetically and a single curve is used in the following analyses.

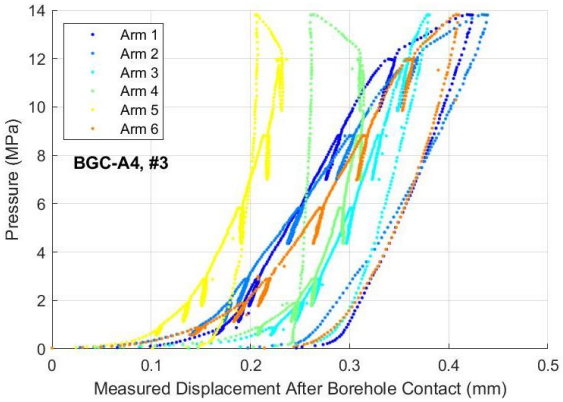

Figure 9. Typical test curves from tests in Borehole BGC-A4

An important step for deriving the true radial displacements in stiff ground is to correct for system compliance. Deformations of membrane and instrument core should both be considered in the correction of data obtained by UofA's probe. A constant system compliance factor calibrated from an inflation test against stiff hollow cylinder is usually used as the correction factor when the pressures are >5 MPa. When the pressures are < 5 MPa a constant value cannot be used and the nonlinearity in calibration data should be treated (Fig 10). This nonlinearity is caused from the length change of the membrane as the ends of membrane are forced into the annulus between probe and cylinder wall [11].

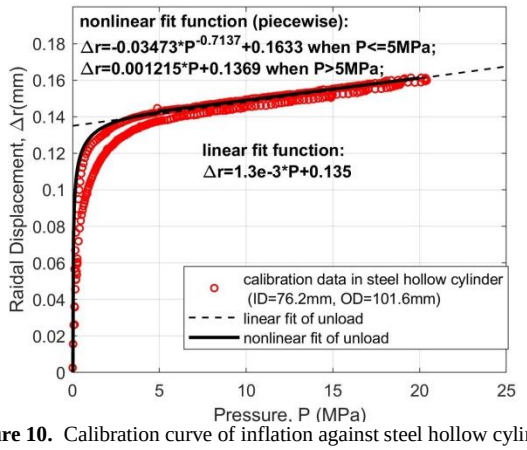

Figure 10. Calibration curve of inflation against steel hollow cylinder

A hysteresis from the load to the unload curve observed in Fig. 10 is a natural response for rubber when it is being stretched, known as Mullin's effect [12]. The stress-strain response of rubber in loading can be partially recovered during the relaxation between tests. In this work, unload data was fitted with a piecewise fit function, which was then applied to correct field measurements.

Fig. 11 is an example of the corrected borehole deformations for the test in Fig.9 using a linear system compliance of 1.3 mm/GPa. Also shown in Fig. 11 is the same data but processed using the calibrated nonlinear system compliance. when only a constant calibration factor was considered, a soft response in the lower expansion range is predicted, and the shear modulus from the unload-reload cycles could be underestimated.

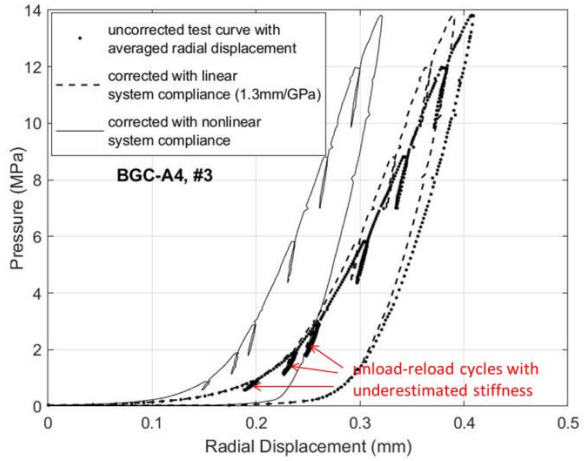

Figure 11. Example of correction of test data for system compliance

3. Strain Dependency of Pressuremeter Shear Modulus

Wroth [13] suggested that the ground stiffness be evaluated using the unload/reload cycles once the membrane has been expanded sufficiently against the borehole wall. This has the advantages over using the initial expansion because: 1) the deformations are likely to be elastic and less affected by the drilling-induced disturbance to the borehole wall, and 2) the stress dependency of stiffness can be assessed with multiple cycles at different pressure levels.

Pressuremeter test data can be interpreted using cylindrical cavity expansion theory assuming that 1) axial strain is zero and 2) borehole deformation is axisymmetric. The statement underlying the second assumption is that material is rotationally isotropic in the testing plane. Therefore, only the averaged displacements are needed for this interpretation.

For testing in linearly elastic materials, the shear modulus G, is directly determined as half of the slope of the unload-reload cycle. However, Giger et al. [6] in their triaxial tests on the Opalinus Clay demonstrated a nonlinear response over small axial strains. The potential impact of this nonlinear response on the interpreted shear modulus was evaluated in the pressuremeter tests. The reduction of radial displacement in unload-reload cycles was kept at 0.01 mm particularly in the 2nd series of tests, so a consistent range of cavity strain ε_c (defined as ratio of radial displacement u to borehole radius r_0, i.e., $\varepsilon_c=u/r_0$) could be used in the evaluation.

In unload, $\Delta\varepsilon_c$ and Δp is calculated using the values taken at the start of the unload (Fig. 12).

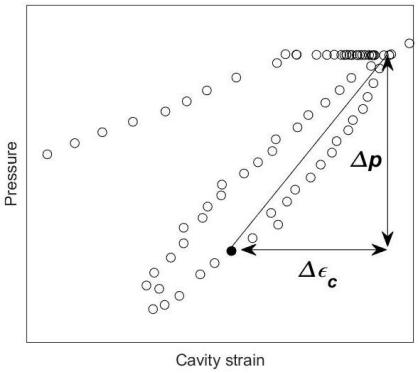

Figure 12. Evaluation of pressuremeter shear modulus using unload data

Following Wood's [14] notation, a pressuremeter shear modulus G_p is defined as the secant relationship of pressure change Δp over the change of cavity strain $\Delta\varepsilon_c$ at borehole wall,

$$G_p = \frac{\Delta p}{2\Delta\varepsilon_c} \tag{1}$$

It should be noted that Eq. (1) was established with two conditions – 1) borehole expansion is small; and 2) that the volumetric strain of the ground is zero, i.e., undrained loading. The hydraulic conductivity of the Opalinus Clay is on the order of 10^{-14} – 10^{-12} m/s [6]. Liu [15] showed that using loading rates 0.45MPa/min and 0.15-0.3 MPa/min for the 1st and 2nd series of tests, respectively, the undrained condition is reasonably satisfied.

A mean value of G_p is usually determined using a linear fit for the stress-strain data points. Alternatively if the data warrants it, the variation of G_p can be derived using a power law function,

$$G_p = \frac{\alpha}{\beta}\Delta\gamma_c^{\beta-1} \tag{2}$$

where $\Delta\gamma_c$ is the shear strain increment at cavity wall and equal to $2\Delta\varepsilon_c$ in an undrained deformation; α and β are material parameters that can be conveniently determined from the plot of $\ln\Delta p$ and $\ln\Delta\gamma_c$. Eq. (2) was proposed by Bolton and Whittle [16] from a power-law relationship between shear stress and shear strain, i.e.,

$\Delta\tau = \alpha\Delta\gamma^{\beta}$. With the nonlinear fit function of G_p, the constitutive relationship between $\Delta\gamma$ and other shear modulus measures (e.g., secant shear modulus) can readily be derived.

G_p was first evaluated using the linear fit and then evaluated using Eq. (2). For the data from tests BGC-2, #2 (Fig. 13) and BGC-A4, #3 (Fig. 14), both located at the deeper level of the boreholes (30 m and 9.7 m, respectively) were used for this evaluation. Typically, data from both reloads and unloads can be used for the analysis. However, reloads from tests in BGC-2 all started from the same pressure level and had minor variation from test to test. Therefore, only results from the analyses of unloading data are presented here. The strain dependency of rock stiffness can be seen from the gradual reduction of G_p in the two tests as $\Delta\gamma_c$ increases. When $\Delta\gamma_c$ is <1e-4, G_p can be as high as over 16 GPa at the first strain increment, while for $\Delta\gamma_c$>1e-4, G_p ranges from 2 to 8 GPa. The reduction in G_p as a function of $\Delta\gamma_c$ can also be quantified by the exponential index β-1 in the fit functions (Fig. 13 and Fig. 14), i.e., the lower β the more nonlinear the G_p variation.

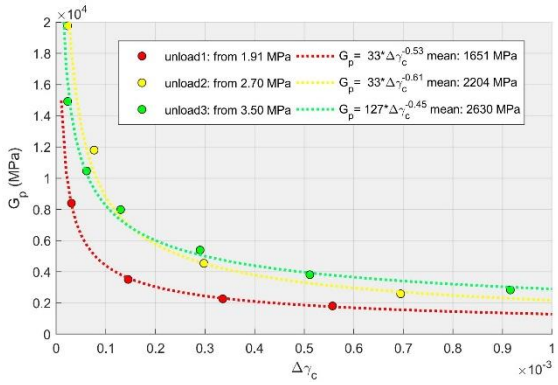

Figure 13. Variation of pressuremeter shear modulus G_p with strain increment from unloads in test BGC-2 #2, 30.0m (shaly facies)

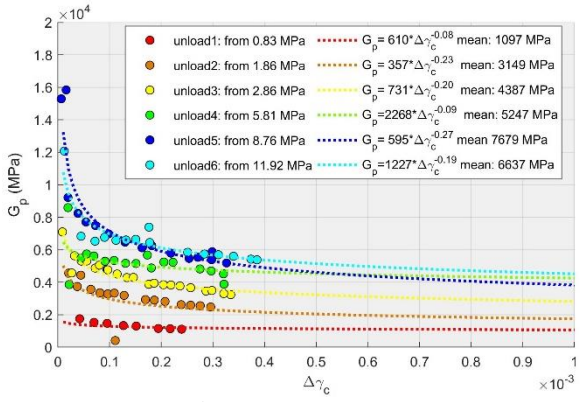

Figure 14. Variation of pressuremeter shear modulus G_p with shear strain increment from unloads in test BGC-A4 #3, 9.7 m (sandy facies)

Inspection of Fig. 13 and Fig. 14 reveals that the fit curves of G_p from BGC-2, #2 are more nonlinear than those from BGC-A4, #2. This difference may be related to differences in the rock facies and/or the difference in the pressure control parameters (e.g., unloading rate, pressure hold duration, etc.) used in the two cases. To investigate the impact of unloading rate, two unloads at different rates were compared in test BGC-A4, #6 (Fig. 15). After the first regular unload-reload cycle, a second cycle using a fast unload (923 kPa/min) was performed after a 1 min pressure hold. The results shown in Fig. 15 indicate that the fast unload tends to promote a stiffer response immediately after the pressure reversal. This suggests that the unloading rate can influence the derived G_p variation.

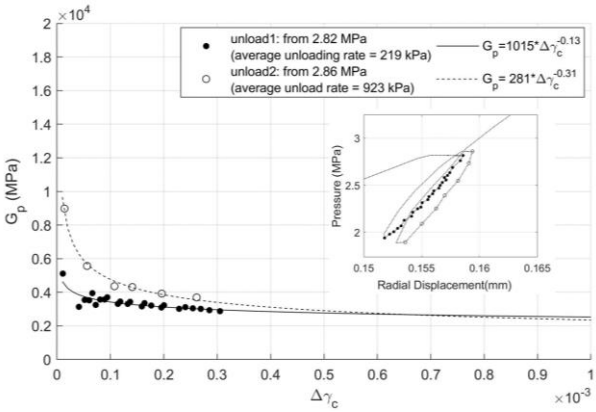

Figure 15. Comparison of G_p variations derived from data (BGC-2 #10, 4.9m) at different unloading rates

4. Stress Dependency of Pressuremeter Shear Modulus

In Fig. 13 and Fig. 14, the mean value of G_p for the given range of shear strain increment in each unload is also determined. It indicates that the derived shear modulus is affected by the pressure where the unload starts. Because G_p also varies with the shear strain, an unbiased way to interpret the stress dependency is to compare G_p at the same shear strain increment $\Delta\gamma_c$.

With the power-law functions of G_p determined from the last section, G_p can readily be evaluated for any $\Delta\gamma_c$. For all the tests, a representative G_p is determined when $\Delta\gamma_c$=1e-4.

The effect of applied stress on rock stiffness can be seen from the variation of the representative G_p with unload starting pressure (Fig. 16). Because of different nonlinearities observed in the two cases, the G_p determined at $\Delta\gamma_c$=1e-4 is systematically higher in the 1st series of tests (Fig. 16 (a)) than that from the 2nd series of tests (Fig. 16 (b)). Nevertheless, data from two series of tests yield the similar trend - in general, G_p increases at a first few unloads. It starts to become less dependent on stress once when pressure reaches a threshold, for example, about 5MPa for tests in BGC-A4. The low G_p at low expansion pressure may indicate the degraded rock stiffness in the near-borehole region after drilling-induced unloading. The gradual increase of G_p before a constant level is reached is likely a process of stiffness recovery associated with micromechanical response of rock pores/cracks under stress. At each pressure increment, an estimation of stiffness variation in radius may be possible with the solution derived by Santarelli et al. [17] for borehole surrounded by pressure-dependent materials. However, the uncertainties in far-field stresses and the stress distribution for an initially unloaded borehole created challenges for a sound interpretation. It was also intended to associate the observed discrepancy between G_p at the same unloading pressure with factors such as rock facies and the test depths, but no obvious correlation could be concluded generally.

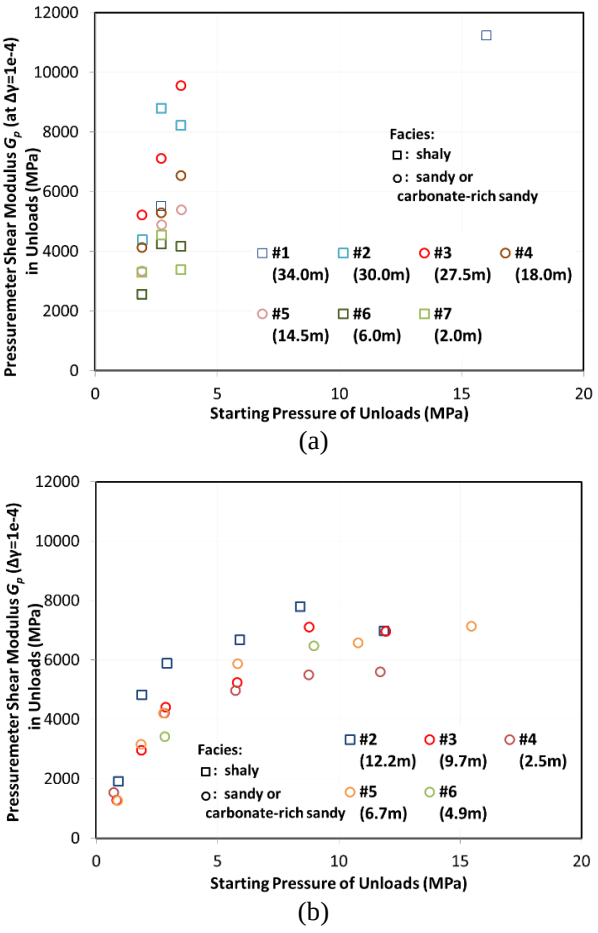

Figure 16. Pressuremeter shear modulus G_p determined from unloads starting at different pressures. G_p was evaluated at $\Delta\gamma$=1e-4 from the power-law fit of unload data for tests in (a) BGC-2 and (b) BGC-A4.

For further investigation, a laboratory study of strain/stress path for pressuremeter testing and its influence on the stiffness evolution of Opalinus Clay is desired. Borehole seismic survey with multiple penetration depths, if available, may lend insights of radial (and possibly circumferential) variation of rock stiffness around the borehole after initial unloading.

5. Conclusions

Data from pre-bored pressuremeter tests at Mont Terri Rock Laboratory were used to derive strain and stress dependencies of shear modulus for the undrained condition. All tests were carried out to ensure the pressuremeter loading was parallel to bedding. All unload-reload cycles in tests revealed a nonlinearity of rock stiffness. This nonlinearity was captured by a power-law function of shear strain increment at borehole wall $\Delta\gamma_c$. With the G_p evaluated at a constant $\Delta\gamma_c$, the relation between rock stiffness and the stress applied on the borehole wall was assessed unbiasedly. A similar trend showing an increase of rock stiffness in the initial loading before a constant level was reached was observed from two series of tests. This relation may be further quantified with laboratory evidences of stiffness evolution under the stress/strain path relevant to pressuremeter testing.

Acknowledgement

The authors would like thank SolExperts for providing field data from tests in borehole BGC-2. The thanks are also extended to Jakob Brandl for his incremental modification of UofA's pressuremeter probe and David Jaeggi from Swisstopo for their helps on site.

6. References

[1] Bossart, P., Bernier, F., Birkholzer, J. "Mont Terri rock laboratory, 20 years of research: introduction, site characteristics and overview of experiments", Swiss J Geosci, 110, pp. 3–22, 2017. https://doi.org/10.1007/s00015-016-0236-1

[2] Morgenstern, N.R. "Instability mechanisms in stiff soils and weak rocks", in: Tenth Southeast Asian Geotechnical Conference, Taipei, China, pp. 27–36. 1990.

[3] Gens, A. "On the hydromechanical behaviour of argillaceous hard soils-weak rocks", in: Proceedings of the 15th European Conference on Soil Mechanics and Geotechnical Engineering. Athens, Greece, pp. 71–118. 2013. https://doi.org/0.3233/978-1-61499-199-1-71

[4] Amann, F., Wild, K.M., Loew, S., Yong, S., Thoeny, R., Frank, E. "Geomechanical behaviour of Opalinus Clay at multiple scales: results from Mont Terri rock laboratory (Switzerland)", Swiss J. Geosci. 110, pp. 151–171, 2017. https://doi.org/10.1007/s00015-016-0245-0

[5] Favero, V., Ferrari, A., Laloui, L. "Anisotropic behaviour of Opalinus Clay through consolidated and drained triaxial testing in saturated conditions", Rock Mech. Rock Eng. 51, pp. 1305–1319, 2018. https://doi.org/10.1007/s00603-017-1398-5

[6] Giger, S.B., Ewy, R.T., Favero, V., Stankovic, R., Keller, L.M. "Consolidated-undrained triaxial testing of Opalinus Clay: Results and method validation", Geomech. Energy Environ. 14, pp. 16–28, 2018. https://doi.org/10.1016/j.gete.2018.01.003

[7] Wild, K.M., Amann, F. "Experimental study of the hydro-mechanical response of Opalinus Clay – Part 1: Pore pressure response and effective geomechanical properties under consideration of confinement and anisotropy", Eng. Geol. 237, pp. 32–41, 2018. https://doi.org/10.1016/j.enggeo.2018.02.012

[8] Corkum, A.G., Martin, C.D. "The mechanical behaviour of weak mudstone (Opalinus Clay) at low stresses", Int. J. Rock Mech. Min. Sci. 44, pp. 196–209, 2007. https://doi.org/10.1016/j.ijrmms.2006.06.004

[9] Wild, K.M., Wymann, L.P., Zimmer, S., Thoeny, R., Amann, F. "Water retention characteristics and state-dependent mechanical and petro-physical properties of a clay shale", Rock Mech. Rock Eng. 48, pp. 427–439. 2015. https://doi.org/10.1007/s00603-014-0565-1

[10] Zalesky, M., Bühler, C., Burger, U., John, M. "Dilatometer tests in deep boreholes in investigation for Brenner base tunnel", in: Barták, Hrdina, Romancov, Zlámal (Eds.), Underground Space – the 4th Dimension of Metropolises, Taylor & Francis Group, Prague, Czech. pp. 283–288. 2007. https://doi.org/10.1201/NOE0415408073.ch47

[11] Clarke, B.G. "Pressuremeters in geotechnical design", CRC Press, 1995.

[12] Bouasse, H., Career, Z. "On the tensile curves of vulcanized rubber", Ann. Fac. Sci. Toulouse Math. Ser. 2, 5, pp. 257–283, 1903. https://doi.org/10.5802/afst.205

[13] Wroth, C.P. "The interpretation of in situ soil tests", Géotechnique, 34, pp. 449–489, 1984. https://doi.org/10.1680/geot.1984.34.4.449

[14] Wood, D.M. "Strain-dependent moduli and pressuremeter tests", Géotechnique, 41, pp. 509–512, 1990. https://doi.org/10.1680/geot.1991.41.4.621

[15] Liu, L., "Numerical study of Reservoir Geomechanical Pressuremeter testing under anisotropic in-situ stresses", M.Sc., University of Alberta, 2015.

[16] Bolton, M.D., Whittle, R.W. "A non-linear elastic/perfectly plastic analysis for plane strain undrained expansion tests", Géotechnique, 49, pp. 133–141, 1999. https://doi.org/10.1680/geot.1999.49.1.133

[17] Santarelli, F.J., Brown, E.T., Maury, V. "Analysis of borehole stresses using pressure-dependent, linear elasticity", Int. J. Rock

Mech. Min. Sci., 23, pp. 445–449, 1986.
https://doi.org/10.1016/0148-9062(86)92310-7